DOI 10.5012/bkcs.2011.32.3.927

Morphology and Charge Transport Properties of Chemically Synthesized Polyaniline-poly(ε-caprolactone) Polymer Films

C. Basavaraja, Dae Gun Kim, Won Jeong Kim, Ji Hyun Kim,† and Do Sung Huh*

Department of Chemistry and Institute of Basic Science, Inje University, Kyungnam 621-749, Korea
**E-mail: chemhds@inje.ac.kr*
†Department of Chemical and Bio-Engineering, Kyungwon University, Seongnam 461-701, Korea
Received November 26, 2010, Accepted January 12, 2011

Conducting polyaniline-poly(ε-caprolactone) polymer composites were synthesized *via in situ* deposition techniques. By dissolving different weight percentages of poly(ε-caprolactone) (PCL) (10%, 20%, 30%, 40%, and 50%), the oxidative polymerization of aniline was achieved using ammonium persulfate as an oxidant. FT-IR, UV-vis spectra, and X-ray diffraction studies support a strong interaction between polyaniline (PANI) and PCL. Structural morphology of the PANI-PCL polymer composites was studied using scanned electron microscopy (SEM) and transmittance electron microscopy (TEM), and thermal stability was analyzed by thermogravimetric analysis (TGA) technique. The temperature-dependent DC conductivity of PANI-PCL polymer composite films was studied in the range of 305-475 K, which revealed a semiconducting behavior in the transport properties of the polymer films. Conductivity increased with the increase of PCL in below critical level, however conductivity of the polymer film was decreased with increase of PCL concentration higher than the critical value.

Key Words : Biodegradable polymers, DC conductivity, Polymer composites, Poly(ε-caprolactone), Polyaniline

Introduction

Intrinsically conducting polymers (ICP), commonly termed as synthetic metals, have been the subject of extensive theoretical and experimental studies. Among the ICPs, polyaniline (PANI) has become the subject of special interest due to its relatively low cost. In the last century, PANI has been described in various forms such as aniline black, emeraldine, nigraniline, etc., that has been prepared either chemically or electrochemically by the oxidation of aniline. The most common green protonated emeraldine has conductivity on a semiconductor level of the order of 10^0 S cm^{-1}, which is greatly higher than that of common polymers (10^9 S cm^{-1}) but lower than that of typical metal (> 10^4 S cm^{-1}). The changes in physicochemical properties of PANI occurring in response to various external stimuli are used in various applications,[1,2] e.g., in organic electrode, sensors, and actuators.[3-5] Other uses are based on the combination of electrical properties typical of semiconductor with materials parameter characteristics of polymer like the development of "plastic" microelectronics,[1,6] electro-chromic devices,[7] tailor-made composite system,[8,9] and "smart" fabrics.[10] The establishment of the physical properties of PANI reflecting the condition of preparation is thus of fundamental importance. The important property of PANI is that it is soluble directly in organic solvent from the oxidized state. The synthetic method using a dopant with a relatively large molecular weight such as dodecylbenzene sulphonic acid (DBSA), camphor sulphonic acid (CSA), and naphthalene sulphonic acid (NSA) reduces the interchain interaction of PANI chains.[11,12]

Poly(ε-caprolactone) (PCL) is attractive due to its low cost, sustained biodegradability, and availability at low molecular weight.[15,16] PCL is a semicrystalline bio-resourceful poly(α-hydroxyester) with an orthorhombic crystal structure.[17,18] Due to its hydrophobic nature and high crystalline degree, PCL degrades slowly[19,20] by hydrolysis and has been considered in a wide range of applications, for example, biodegradable packaging materials, implantable biomaterials, scaffold, and micro-particles for drug delivery.[21-23] The crystallization behavior of PCL blends has been investigated in a number of studies.[24,25] Moreover, the effect of reinforcement materials such as starch, clay, and single-walled nanotubes, on the crystallization of PCL has been studied *via* isothermal and non-isothermal crystallization.[26,27] Behavior during non-isothermal crystallization is of great importance in the production of composites based on semi-crystalline polymers such as PCL because crystallization has a great effect on the physical properties of the composite.[27]

In the quest for better materials, considerable research attention has been focused over the past few years on the modification of specialty vinyl addition polymers and condensation polymers, particularly delving into ways to improve their bulk properties.[28-32] One of the important advancements in this direction is the preparation of the hybrid nanocomposite materials of these polymers with selective inorganic/organic components.[33-37] Yet another avenue of research that has been successful to a certain extent is the search for biodegradable materials that can be

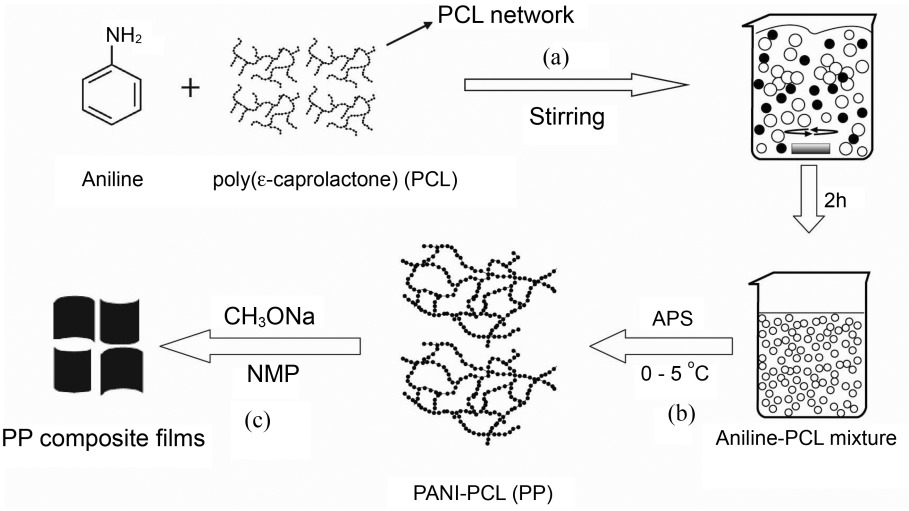

Figure 1. Schematic diagram representing the polymerization of PANI in the presence of PCL to form PANI-PCL composite. (a) Start of reaction with stirring the mixture of aniline and PCL to form aniline-PCL complex, (b) followed by the polymerization of aniline in the complex to form PANI-PCL composite, and (c) shows the formation of composite films.

successful replacements for synthetic polymers while also serving as better alternatives for plastic wastes. These biodegradable polymers are produced from renewable resources, such as plants, animals, and microbes, through biochemical reactions, offering a convenient and environment-friendly solution to the problem of plastic wastes. In this regard, natural fibers have emerged as renewable and biodegradable natural cellulose materials. Despite their relatively modest strength and low density, plant fibers have been found to be capable of producing fibrous composites with high-specific strength. They are becoming increasingly useful as raw materials for the preparation of cost-effective and environment friendly composite materials.

In our earlier studies we have chosen some biopolymers such as polymannuronate and alginate to synthesize new conducting composites with PANI and polypyrrole (PPy). After characterization of the composites, physico-chemical properties including solubility, conductivity, and microwave absorption ability, etc. have been studied.[28-37] It was found that there has been an increase in these properties of the conducting polymers (PANI and PPy) after the formation of composites with the above biopolymers. It is for the reason that an effort has been made to synthesize new PANI composites with PCL.

The major aim of this study is to increase the physico-chemical functionalities of conducting PANI by incorporating biodegradable PCL into the PANI polymer matrix. PANI-PCL polymer composites were synthesized by *in situ* polymerization of aniline using different weight percentages (wt %) of PCL. The synthesized polymer composites were characterized by FTIR, UV-vis spectra, and XRD studies. The surface morphology was characterized by SEM and TEM techniques, and the thermal stability by TGA. Temperature-dependent DC conductivity studies were performed to understand the conduction mechanism in the PANI-PCL (PP) polymer composites.

Experimental

Materials. AR-grade aniline, poly(ε-caprolactone), and ammonium per sulfate (APS) were purchased from Sigma-Aldrich, and *N*-methyl-2-pyrrolidinone (NMP) was obtained from Junsei Chemical Co. The purchased reagents were used without further purifications. All solutions were prepared in aqueous media utilizing deionized water.

Synthesis of PANI and PP Polymer Composites. Figure 1 shows the schematic diagram of the synthetic procedure for the formation of PP polymer composites. Aniline and PCL were combined in aqueous media in a 500 mL beaker and stirred continuously at 500 rpm for about 2 h. After stirring, the aqueous solution turned a light brown color as the aniline monomer formed a complex with PCL. The solution was cooled to 0-5 °C with continued stirring. APS was consequently added by drop-wise with continuous stirring for about 5 h to form a light green PANI polymer composite. The precipitated powder was filtered and washed with distilled water and methanol until the filtrate became colorless. It was then dried in a vacuum at room temperature for 24 h. The target mass loading of PCL in the polymer composites was varied as 10%, 20%, 30%, 40%, and 50%. The polymer composites are denoted as PP-10, PP-20, PP-30, PP-40, and PP-50, respectively. Pure PANI was synthesized in this manner without the addition of PCL.

For the preparation of thin films of PANI and PP composites, the powder was treated with a solution of sodium ethoxide (C_2H_5ONa) and ethanol, and was magnetically stirred at room temperature for 12 h. Finally, the precipitate was filtered and washed repeatedly with ethanol and stored in a desiccator for 4 h at room temperature. About 2 g of obtained powder was taken in 30 mL of NMP solution, magnetically stirred for 24 h at room temperature. The solution was then placed on a Petri dish, and the NMP solvent was allowed to evaporate at 45 °C for 48 h. The

obtained films were then placed in distilled water, rinsed with ethanol, and dried at room temperature for another 24 h. To obtain solvent-free films, the residual NMP was removed by three cycles of doping using 1 M HCl solution for 18 h and de-doped by 0.1 M NH_4OH solution for another 18 h at room temperature. The resulting NMP-free composite films were cleaned in deionized water and dried at room temperature for about one day.[28-34]

Characterization and Property Evaluation of the Composites. The characterization of the composites was described in earlier studies.[28-37] The FT-IR spectra of the samples were measured by a Perkin Elmer (model 783) IR spectrometer in KBr medium at room temperature. The UV-vis spectra were recorded by a Shimadzu UV-vis-NIR spectrophotometer (UV-3101PC) in chloroform. The XRD patterns were obtained using a Philips Diffractometer (PW 1710) with Cu-Kα (λ = 1.5406 Å) radiation. The diffractograms were recorded in terms of 2θ in the range of 5-80° at a scanning rate of 2° per min. Thermal properties were obtained by TGA (Perkin Elmer model TGA 7) in the range 20 to 800 °C at 2 °C /min in nitrogen atmosphere. The morphology of the synthesized composite films was investigated by using SEM (Philips XL-30 ESEM). The samples for SEM were mounted on aluminum studs using an adhesive graphite tape and were sputter-coated with gold before analysis. The DC electric measurements of the obtained composite films were performed within the temperature range of 300 to 500 K using the four-probe technique with a Keithly 224 constant current source and a Keithly 617 digital electrometer.

Results and Discussion

Characterization of PANI and PANI-PCL (PP) Polymer Composites. The infrared (FT-IR) spectra of PCL, PANI, and composites of PP-30 and PP-50 powders are given in Figure 2. Figure 2(a) shows for PCL, and 2(b) shows for PANI, PP-30, and PP-50. The PANI spectrum is similar to those reported in earlier studies.[32,33,36,37] The characteristic transmittance bands of pure PANI are observed at 1550 cm^{-1} (C=C stretching of quinoid ring), 1469 cm^{-1} (C=C stretching of benzenoid ring), 1243 and 1296 cm^{-1} (C-N stretching), and 797 and 1128 cm^{-1} (C-H stretching). The presence of transmittance bands at 797 cm^{-1} is attributed to *para*-substituted aromatic rings. The broad transmittance band at 1128 cm^{-1} is characteristic of protonated emeraldine salt in acidic media; this indicates high electronic conductivity and high degree of electronic delocalization.[38]

The transmittance peaks located at 2942, 2862, and 1723 cm^{-1} for PCL were assigned as the stretching vibration of $–CH_2$ and vibration of –C=O bonds, respectively.[38-40] Polymer composite PP-30 shows transmittance bands at 2852, 3055, and 1711 cm^{-1}, whereas PP-50 has peaks at 3005, 2845, and 1701 cm^{-1}. The other bands for PANI in the polymer composites remain more or less the same with a small shift in their transmittance peaks.

Figure 3 shows the UV-vis spectra for pure PANI and composites of PP-30 and PP-50 in 1 mg/mL NMP solution. As expected from literature, PANI shows three peaks at around 250 and 400 nm, and a fairly broad peak at around 600 nm.[32] These bands are due to $\pi \rightarrow \pi^*$ and n $n \rightarrow \pi^*$ transitions, which are attributed to benzenoid and quinoid excitement absorption, respectively. As PCL concentration increased in the PANI-PCL polymer composites, the peak around 600 nm disappears and the peak at 250 nm becomes sharper. The spectra for PP-30 show only a sharp peak at 250; the peak at 400 nm which appears for PANI has disappeared. This is the same case in PP-50, however, the peak due to benzenoid excitement absorption further sharpened compared with PP-30.

FTIR and UV-vis spectra for PP-10 and PP-40 were similar to PANI and PP-50, respectively. This similarity

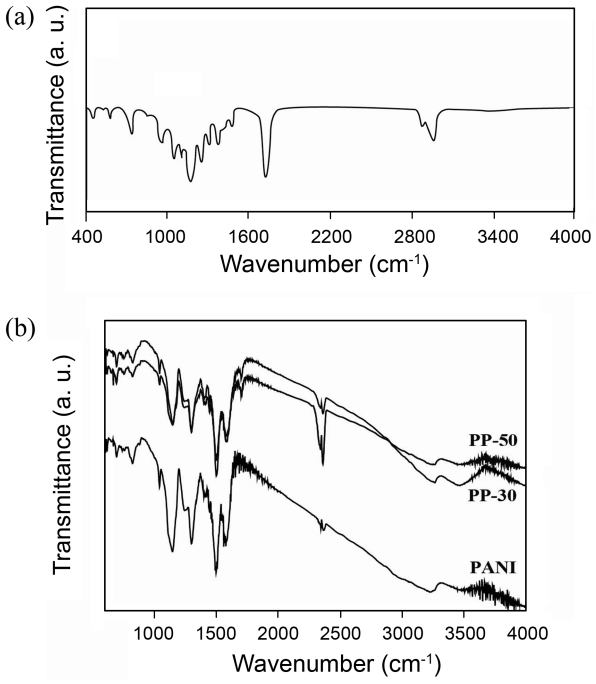

Figure 2. FTIR spectra for PCL (a), (b) PANI, PP-30 and PP-50.

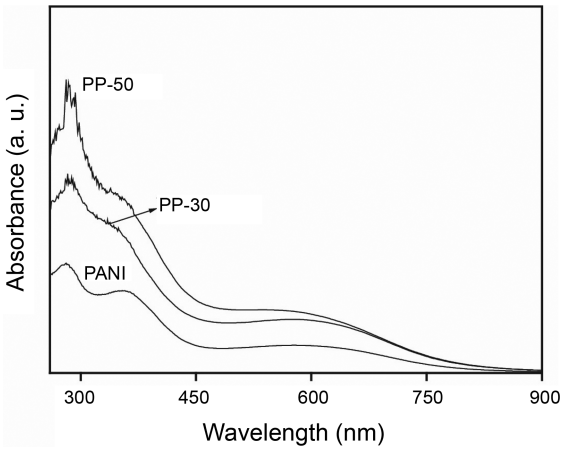

Figure 3. UV-vis spectra for PANI and the composites of PP-30 and PP-50.

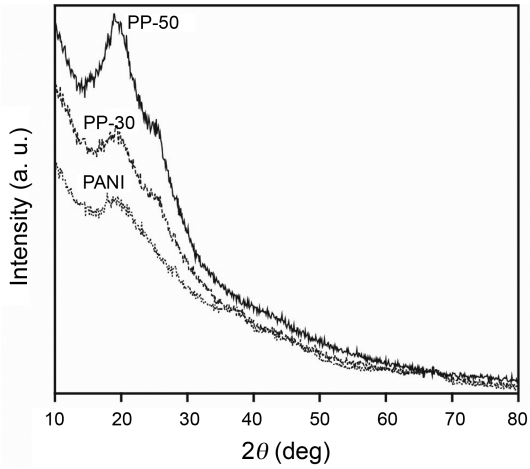

Figure 4. XRD-patterns for PANI and the composites of PP-30 and PP-50.

indicates conjugation between PANI and PCL, which, in turn, implies the formation of PANI-PCL polymer composite.

Figure 4 shows XRD patterns for PANI and the composites PP-30 and PP-50. The diffraction pattern for PANI shows a slightly broad peak at 25°, which is a characteristic peak for PANI.[32,41] The same peak becomes sharper as the PCL concentration increases in the PP polymer composites, as observed in PP-30, and PP-50. There is also an appearance of a secondary peak at 30° in the composites that is absent in PANI; this peak may be due to PCL. Thus, as PCL concentration increases, the composites obtain a more crystalline nature. In the spectral characterization, the shift in FTIR peaks, the disappearance of the quinoid band in the UV-vis spectra, as well as the sharpening of peaks in the XRD patterns of the composites suggest that PANI-PCL composite was formed in this experimental process.

Surface Morphology of PANI-PCL Polymer Composites. Figure 5 shows SEM images for the polymer films of PP-10 (a), PP-30 (b), and PP-50 (c) obtained at 5 μm. Image (d)

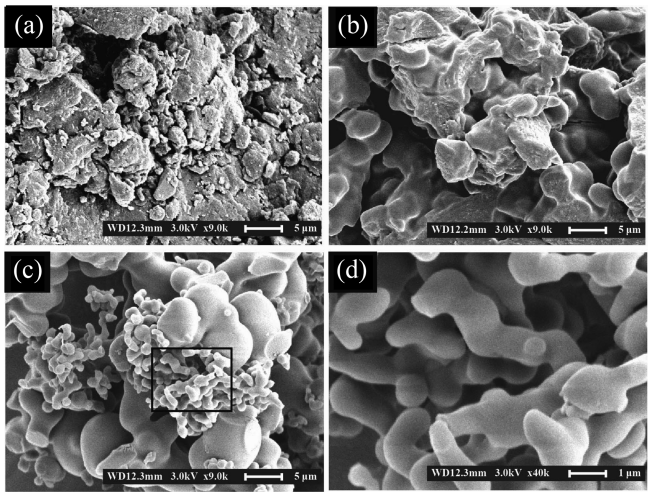

Figure 5. SEM images for PP-10 (a), PP-30 (b), and PP-50 (c); (d) shows an extended part of the rectangle in (c).

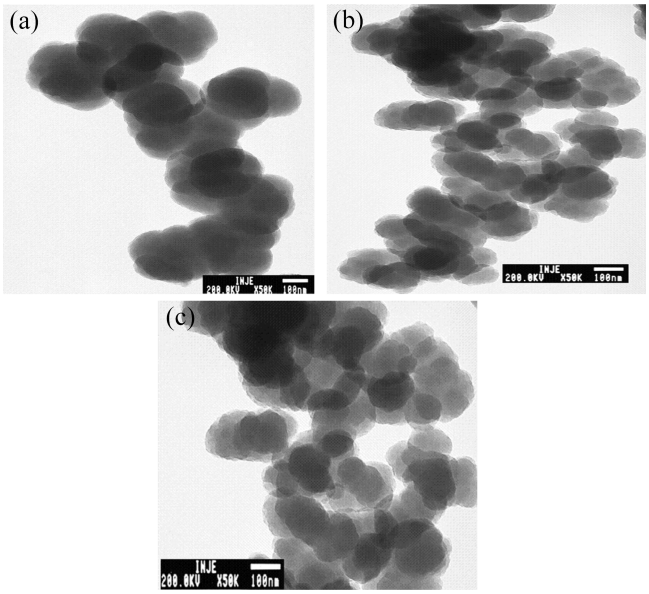

Figure 6. TEM images for PP-10 (a), PP-30 (b), and PP-50 (c) polymer composites.

shows an extended image of the rectangle in (c), which is obtained at 1 μm. PP-10 shows non-uniform lump-like structures that appear all over the surface of the polymer films; this result is similar to earlier reports.[37,41] The surface image of PP-30 shows a mixture of both gel- and lump-like structures which appear combined. In PP-50, there is a complete disappearance of the lumps. Formation of a gel-like structure appears to be predominant over the lump structure. A finger-like structure is also observed in (c) and in the extended image (d).

Figure 6 presents the TEM images of the surface microstructure for the polymer composites of PP-10 (a), PP-30 (b), and PP-50 (c). The image of PP-10 shows particles in spherical form with dimensions of 50 nm. As PCL concentration increases in the polymer composites, the spherical particles merge to form an aggregate structure with a particle size about 10-20 nm. After the formation of polymer composites, the particle size decreases in dimensions and merges to form smaller aggregates.[42,43] The morphological changes in the polymer blends may be attributed to the presence of PCL, as evidenced by SEM and TEM image analysis of the polymer films.[41]

TGA Analysis for PANI, PANI-30, and PANI-50. TGA is one of the most useful techniques for evaluating the onset of thermal decomposition temperature and determining the thermal stability of conducting polymers. Figure 7 shows TGA curves for PCL and PANI, also for the polymer composites PP-30 and PP-50. The TGA curve for PCL exhibit four different stages at different temperature ranges. From room temperature to 120 °C may be due to the loss of moisture or some sort of impurities present in the polymer, from 120 °C - 400 °C is may due to the loss of dopant ions and follows a loss of polymer backbone between 450 °C to 600 °C. From 600 °C - 800 °C a complete degradation of organic polymer moieties present in the polymer occurs. The

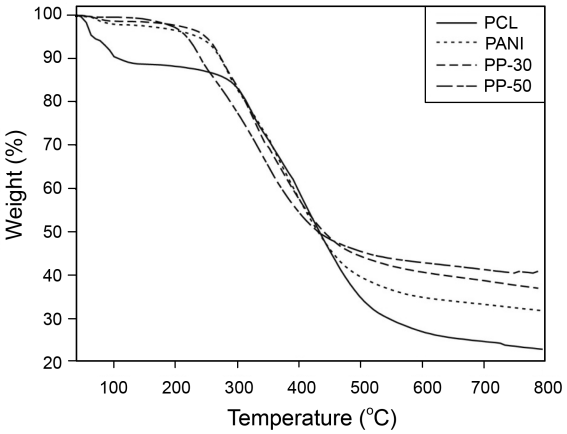

Figure 7. TGA curves for PCL and PANI, and the composites PP-30 and PP-50.

TGA results obtained from PANI[42,43] suggest that the initial stages of weight loss are due to the volatilization of water molecules; at higher temperatures, breakage of the polymeric backbone and dopant moieties occur, and at more extreme temperatures, the residues in the region are mainly thermally stable, inert materials like minerals and metallic impurities. The initial stage in these polymer composites corresponds to that of the moisture/water molecule in the polymer composites. The second loss around 250-500 °C is due to thermo-chemical decomposition of the chemically active organic materials within this range. The third stage in the range 500-800 °C implies a complete decomposition of organic polymers present in the polymer composites. If we compare the TGA curves between PCL and PANI, PANI seems to be more stable than PCL. The lower thermal stability of PCL than PANI especially affects to the thermal stability of PP composites at lower temperature in the second range around 200-300 °C. In the temperature range, PP-50 degrades more rapidly than PANI and PP-30. However, the thermal stability turns over smoothly with increasing temperature. The polymer composites of PP-30 and PP-50 show thermally more stability than PANI in the temperature range higher than 400 °C. This may be due to the formation of a new PANI-PCL network in the polymer composite which might cause the increase of the thermal stability in spite the PCL is less thermally stable than PANI. The increased thermal stability of the PANI-PCL polymer composites at higher temperature has reached the peak at the third stage in the range 500-800 °C. The remained weight % is highest in the PP-50. This may be due to the formation of a strong new PANI-PCL network which is not easily degradable at higher temperature. TGA data reveal that PANI-PCL polymer composites have good thermal stability at higher temperature, making them good candidates for melt blending, not only with conventional thermoplastics such as polyethylene, polypropylene, and polystyrene, but also with engineering thermoplastics like polyamides, polyester, and polycarbonates.

Temperature-Dependent DC Conductivity. Figure 8(a) shows the temperature-dependent conductivity for PANI and PANI-PCL composites films, and 8(b) shows the variation of conductivity with PCL wt % in the PANI-PCL films at 313, 403, and 473 K. A steady increase in conductivity clearly occurs with an increase in temperature for all the polymer blends and PANI. The conductivity values increase for a particular concentration of PCL, and further increase in PCL causes a decrease in conductivity to values even less than that of pure PANI. If we observe the Figure 8(a), the increase in conductivity value for both PANI and PP-30 are linear. However this is not the case with PP-40 and PP-50. This means that the increase in conductivity for PP-40 from room temperature to ~390 K is linear, after this temperature there is a sudden increase in the value in the form of jerk and

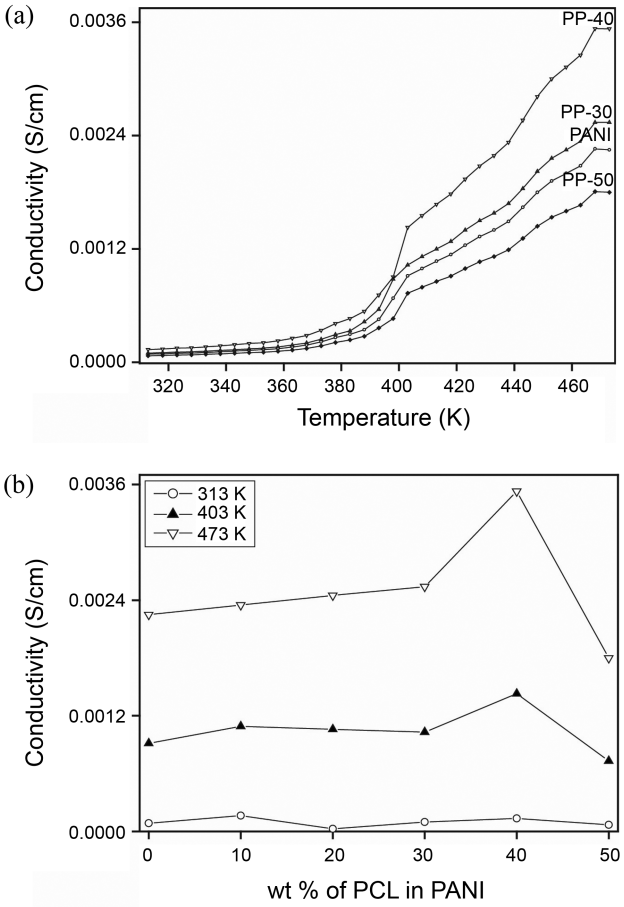

Figure 8. (a) Temperature-dependent conductivity of PANI and PANI-PCL polymer films, (b) variation of conductivity with PCL wt % in the PANI-PCL polymer films at 313, 403, and 473 K.

Table 1. Values of conductivity (S/cm) for PANI and PANI-PCL polymer composites at three different temperatures

Temperature (K)	Conductivity (S/cm) values for PANI and PP polymer composites			
	PANI	PP-10	PP-30	PP-50
313	8.62×10^{-5}	9.7×10^{-5}	1.35×10^{-4}	6.89×10^{-5}
403	9.14×10^{-4}	0.00103	0.00143	7.312×10^{-4}
473	0.00225	0.00254	0.00353	0.0018

this jerk is also observed in small between 390-410 K after which the increase in the conductivity is more or less linear. This jerk observed in PP-50 is small comparing to PP-40 observed at around 400 K and followed by a linear increase. Therefore, temperature dependent conductivity for PP-30 and PP-40 is higher than PANI in spite PP-50 is lower than that of PANI. Table 1 shows the conductivity values at given temperatures for PANI and PANI-PCL polymer composites. The table shows a clear decrease in conductivity values for PP-50.

To explain the temperature-dependent conductivity behavior of the PANI-PCL polymer composites, polymer chains are assumed to extend through the disordered regions and to connect crystalline islands. In this arrangement, the charge carriers may diffuse along the electrically isolated disordered chains, but are always available for localization because of the one-dimensional (1D) nature of the chains.

The temperature-dependence of conductivity for PANI and PANI-PCL polymer composites may be explained on the basis of quasi one-dimensional variable hopping.[44,45] Within the framework of this model, the conductivity is given by the relationship

$$\sigma_{dc} = \sigma_o \exp\left[-(T_o/T)^{\gamma}\right] \quad (1)$$

with $\gamma = 0.5$ for 1D hopping, the quantity σ_o is also temperature-dependent, but the dependence may be neglected when compared to the stronger dependence of the exponential term. T_o is given by the relationship;

$$k_B T_o = 16/L_{||} N(E_F)\, z \quad (2)$$

where $L_{||}$ is localization length, $N(E_F)$ is the density of states at the Fermi level, and z is the number of nearest neighbor chains. T_o is the energy barrier for electrons to hop between localized states. To fit the experimental σ_{dc} data for PANI as in Figure 9, T_o = 6200 K is used in Eq. (1). The figure illustrates a very good agreement between the experimental data and the theoretical straight line. For PP-30 and PP-40 polymer composites, the best fit was achieved using T_o = 6600 K and 6800 K, respectively. This increase in T_o was

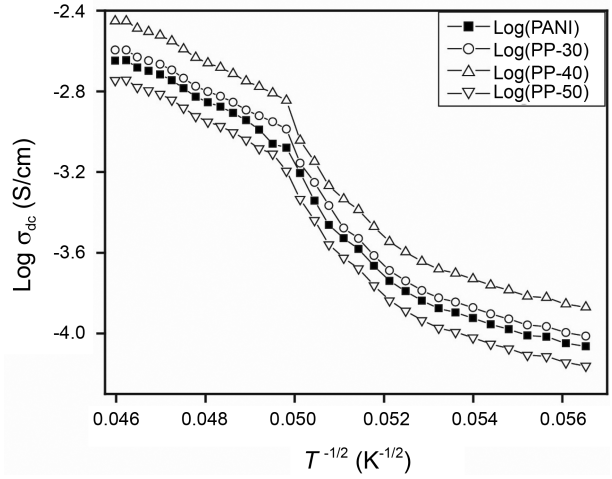

Figure 9. Log conductivity (σ_{dc}) versus $T^{-1/2}$ ($K^{-1/2}$) for PANI and PANI-PCL polymer composites.

expected to increase PCL concentration in PANI. T_o is inversely proportional to the localization length $L_{||}$; so as PCL increases, $L_{||}$ for the charge carriers in the polymer composites decreases. As a result, the charge carriers become more localized and thus less free to move. In terms of T_o, further addition of PCL in PANI increases the energy barrier required for the hopping of electrons, thus making conduction less easy. Therefore, quasi 1D hopping is the mechanism responsible for electrical conductivity in PANI-PCL polymer composites.

The results obtained in this study are a little different from those in earlier studies where PANI was doped with other polymer or biopolymers, and similar to the results observable in some amorphous and porous heterogeneous crystalline solids,[46,47] which are semi-conducting in nature, as well as in some PANI composites.[48,49] In heterogeneous crystalline solids,[46] the decrease in conductivity is accounted for by the destruction of residual crystalline phase. In this case, the introduction of donor or acceptor impurities increases conductivity once the structural phase transition has occurred and the amorphous phase becomes prevalent in the sample. Further increase in such impurities causes a transition that is accompanied by the decrease in conductivity values. The decrease in conductivity in PANI composites[45] may be due to blockage of the conduction path by heterogeneous/metal-like nano-sized particles embedded in the PANI matrix, a relatively high concentration of which makes the hopping process between chains more difficult, thus reducing in conductivity.[45-51]

In a similar fashion the use biopolymers as in our earlier research,[28-30,34,35] it is expected that the conductivity values should increase. Despite increasing the concentration of the biopolymer (PCL), the conductivity increases for a particular concentration (10-40 wt %) and further increase in the same causes the decrease in the conductivity. As there will be microscopic and macroscopic mechanism that will be undergoing in the polymer composite during the conducting process and though several mechanisms have been proposed, it is very difficult to point out the exact mechanism for the decrease in the conductivity data with increase in the temperature.[46-49] Therefore we can suggest that the lowest conductivity in PP-50 in spite of the highest concentration (wt %) of PCL may be due to particle blockage conduction path by PCL (nano size particle) embedded in PANI matrix. It means that the concentration is above the critical value. Also, increase in the concentration of PCL leads to an increasing inter chain distance, which makes hopping between chains more difficult, resulting in reduction of conductivity.

The composition of the polymer composites corresponding to maximum conductivity is the optimum ratio of the two polymeric species PANI and PCL. Outside the optimum ratio, a decrease in conductivity is observed in the respective areas, which is caused either by the decrease in the availability of doping centers (PANI) in the composites[48] or by the hindered movement of ions at a given composition of the polymer composites.[52] In this case, PCL can act as both

enhancer and inhibitor. In PANI-PCL polymer composites, a certain amount of PCL enhances the conductivity for a particular concentration, above which the conductivity of the polymer composites decreases.

Conclusion

In this study, polymer composites containing PANI and PCL were synthesized by *in situ* polymerization using different concentrations of PCL. The morphological study reveals modification of the composites from lumps to a gel-like surface that signifies modification of the composites. The sharpening of XRD peaks and the significant shift in the characteristic bands/peaks of UV-vis and FTIR spectra for the PANI-PCL polymer composites indicate a considerable interaction between PANI and PCL. The thermal data suggest that PANI-PCL polymer composites have good stability around 300 ^{o}C, indicating possible usage for melt blending with engineering thermoplastics. Polymer composites also show appreciable electrical conductivity. The incorporation of a low-cost, biodegradable material PCL polymer is very useful in the development of new biomaterials that may be helpful in the biological system. The method highlights the cost-effectiveness and simplicity of the composite preparation. Improvements in both the physical and electrical properties of the composite can make it more significant for application in the field of polymers.

Acknowledgments. This work was supported by the 2010 Inje University research grant.

References

1. Levi, B. G. *Phys. Today* **2000**, *53*, 19.
2. MacDiarmid, A. G. *Angew. Chem. Int. Ed.* **2001**, *40*, 2581.
3. Jin, Z.; Su, Y.; Duan, Y. *Sens. Actuators B* **2001**, *72*, 75.
4. Sotomayor, P. T.; Raimurdo, I. M.; Zarbin, J. G.; Rohwedder, J. J. R.; Netto, G. O.; Alves, O. L. *Sens. Actuators B* **2001**, *74*, 157.
5. Kane-Maguire, L. A. P.; Wallsce, G. G. *Synth. Met.* **2001**, *119*, 39.
6. Hamers, R. J. *Nature* **2001**, *412*, 489.
7. Rosseinsky, D. R.; Mortimer, R. J. *Adv. Mater.* **2001**, *13*, 783.
8. Kim, G. H. *Macromol. Res.* **2004**, *12*, 564.
9. Cha, S. H.; Kim, J. U.; Lee, J. C. *Macromol. Res.* **2008**, *16*, 711.
10. El-Sherif, M. E.; Yuan, J.; MacDiarmid, A. G. *J. Intell. Mater. Syst. Struct.* **2000**, *11*, 407 .
11. Mallik, H.; Sarkar, A. *J. Non-Cryst. Solid.* **2006**, *352*, 795.
12. Tiwari, A. *J. Poly. Res.* **2008**, *15*, 337.
13. Basavaraja, C.; Jo, E. A.; Kim, B. S.; Mallikarjun, H.; Huh, D. S. *Bull. Korean Chem. Soc.* **2010**, *31*(10), 2967.
14. Basavaraja, C.; Veeranagouda, Y.; Lee, K.; Pierson, R.; Huh, D. S. *Bull. Korean Chem. Soc.* **2008**, *29*, 1.
15. Elfick, A. P. D. *Biomaterials* **2002**, *23*, 4463.
16. Kim, H. W.; Deng, Y.; Miranda, P.; Pajares, A.; Kim, D. K.; Kim, H. E.; Lawn, B. R. *J. Am. Ceram. Soc.* **2001**, *84*, 2377.
17. Ciardelli, G.; Chiono, V.; Vozzi, G.; Pracella, M.; Ahluwalia, A.; Barbani, N.; Cristallini, C.; Giusti, P. *Biomacromlecules* **2005**, *6*, 1961.
18. Lovinger, A. J.; Han, B. J.; Padden, F. J.; Mirau, P. A. *J. Polym. Sci. B: Polym. Phys.* **1993**, *31*, 115.
19. Martin, D. P.; Williams, S. F. *Biochem. Eng. J.* **2003**, *16*, 97.
20. Messersmith, P. B.; Giannelis, E. P. *J. Polym. Sci. A* **1995**, *33*, 1047.
21. Pektok, E.; Nottelet, B.; Tille, J. C.; Gurny, R.; Kalangos, A.; Moeller, M.; Walpoth, B. H. *Circulation* **2008**, *118*, 2563.
22. Aishwarya, S.; Mahalakshmi, S.; Sehgal, P. K. *J. Microencapsul.* **2008**, *25*, 298.
23. Chynoweth, K. R.; Stachurski, Z. H. *Polymer* **1986**, *27*(12), 1912.
24. Skoglund, P.; Fransson, A. *J. Appl. Polym. Sci.* **1996**, *61*(13), 2455.
25. Wang, Y.; Rodriguez-Perez, M. A.; Reis, R. L.; Mano, J. F. *Macromol. Mater. Eng.* **2005**, *290*(8), 792.
26. Homminga, D.; Goderis, B.; Dolbnya, I.; Groeninckx, G. *Polymer* **2006**, *47*(5), 1620.
27. Mitchell, C. A.; Krishnamoorti, R. *Polymer* **2005**, *46*(20), 8796.
28. Basavaraja, C.; Veeranagouda, Y.; Lee, K.; Vishnuvardhan, T. K.; Pierson, R.; Huh, D. S. *J. Polym. Res.* **2010**, *17*, 233.
29. Basavaraja, C.; Jo, E. A.; Kim, B. S.; Huh, D. S. *Bull. Korean Chem. Soc.* **2010**, *31*(8), 2207.
30. Basavaraja, C.; Veeranagouda, Y.; Kim, N. R.; Jo, E. A.; Lee, K.; Huh, D. S. *Bull. Korean Chem. Soc.* **2009**, *30*(5), 1097.
31. Basavaraja, C.; Veeranagouda, Y.; Lee, K.; Pierson, R.; Revanasiddappa, M.; Huh, D. S. *Bull. Korean Chem. Soc.* **2008**, *29*(12), 2423.
32. Basavaraja, C.; Veeranagouda, Y.; Lee, K.; Pierson, R.; Huh, D. S. *J. Polym. Sci. B: Polym. Phys.* **2009**, *47*, 36.
33. Basavaraja, C.; Kim, N. R.; Jo, E. A.; Huh, D. S. *Macromol. Res.* **2010**, *18*(3), 222.
34. Basavaraja, C.; Jo, E. A.; Kim, B. S.; Huh, D. S. *Chem. Phys. Lett.* **2010**, *492*, 272.
35. Basavaraja, C.; Kim, N. R.; Jo, E. A.; Huh, D. S. *J. Polym. Res.* **2010**, *17*, 861.
36. Basavaraja, C.; Jo, E. A.; Kim, B. S.; Kim, D. G.; Huh, D. S. *Polym. Eng. Sci.* **2011**, *51*, 54.
37. Basavaraja, C.; Pierson, R.; Vishnuvardhan, T. K.; Huh, D. S. *Eur. Poly. J.* **2008**, *44*, 1556.
38. Hoidy, W. H.; Ahmad, M. B.; Al-Mulla, E. A. J.; Bt Ibrahim, N. A. *J. Appl. Sci.* **2010**, *10*(2), 97.
39. Venugopal, J.; Zhang, Y. Z.; Ramakrishna, S. *Nanotechnology* **2005**, *16*, 2138.
40. Xiao, X.; Liu, R.; Tang, X. J. *Mater. Sci: Mater. Med.* **2009**, *20*, 691.
41. Basavaraja, C.; Pierson, R.; Huh, D. S. *J. Appl. Polym. Sci.* **2008**, *108*, 1070.
42. Patil, S. F.; Bedekar, A. G.; Agashe, C. *Mater. Lett.* **1992**, *14*, 307.
43. Derval, S. R.; Rosa, S.; Cristina, G. F.; Andréa, G. P. *Polimeros: Cienicia e Technologia* **2004**, *14*(3), 181.
44. Wang, Z. H.; Scherr, E. M.; MacDiarmid, A. G.; Epstein, A. J. *Phys. Rev. B* **1992**, *45*, 4190.
45. Zuo, F.; Angelopoulos, M.; MacDiarmid, A. G.; Epstein, A. J. *Phys. Rev. B* **1987**, *36*, 3475.
46. Ansari, R.; Price, W. E.; Wallace, G. G. *Polymer* **1996**, *37*, 917.
47. Shevaleevskiy, O. I.; Myong, S. Y.; Lim, K. S.; Miyajima, S.; Konagai, M. *Semiconductors* **2005**, *39*(6), 709.
48. Stutzmann, M.; Brandt, M. S.; Bayerl, M. W. *J. Non-cryst. Solids* **2000**, *1*, 266.
49. Raghavendra, S. C.; Khasim, S.; Revanasiddappa, M.; Ambika Prasad, M. V. N.; Kulkarni, A. B. *Bull. Mater. Sci.* **2003**, *26*(7), 733.
50. Su, S. J.; Kuramoto, N. *Synth. Met.* **2000**, *114*, 147.
51. Güven, O. *Radiation Physics and Chemisty* **2007**, *76*, 1302.
52. Ekramul Mahmud, H. N. M.; Kassim, A.; Zainal, Z.; Yunus, W. M. M. *Science Asia* **2005**, *31*, 313.